PERIÓDICO TCHÊ QUÍMICA
ARTIGO ORIGINAL

INVESTIGAÇÃO DO DESEMPENHO TÉRMICO-EXERGÉTICO DE UM AQUECEDOR SOLAR DE AR DE BAIXO CUSTO CONSTRUÍDO COM MATERIAIS LOCALMENTE DISPONÍVEIS

A THERMAL –EXERGY PERFORMANCE INVESTIGATION OF A COST-EFFECTIVE SOLAR AIR HEATER CONSTRUCTED FROM LOCALLY AVAILABLE MATERIALS

تحليل الأداء الحراري والإكسرجي لسخان هواء شمسي منخفض التكلفة مصنع من مواد متوفرة محلياً

Ali Al-Jubainawi *
University of Misan, College of Engineering, Department of Mechanical Engineering, Iraq. ORCID: 0000-0002-0849-1751

Mahmood S. Mahmood
University of Misan, College of Engineering, Department of Mechanical Engineering, Iraq. ORCID: 0009-0006-2149-5235

Mohammed Abbas
University of Misan, College of Engineering, Department of Mechanical Engineering, Iraq. ORCID: 0009-0001-6024-7078

Abbas Bleash
University of Misan, College of Engineering, Department of Mechanical Engineering, Iraq. ORCID: 0009-0000-6988-2310

Mustafa Ajeal
University of Misan, College of Engineering, Department of Mechanical Engineering, Iraq. ORCID: 0009-0002-3427-8791

** Corresponding author*
e-mail: alihussein.mcm@uomisan.edu.iq

Received 10 October 2025; received in revised form 19 January 2026; accepted 22 February 2026

RESUMO

Introdução: Os aquecedores solares de ar (ASAs) representam uma tecnologia solar passiva promissora para aplicações de aquecimento de ambientes e secagem. Apesar de seu potencial, a combinação da avaliação de desempenho térmico (primeira lei) e exergético (segunda lei) de ASAs fabricados com materiais de baixo custo e localmente disponíveis ainda é pouco explorada. **Objetivo**: Este estudo teve como objetivo projetar, construir e avaliar experimentalmente três configurações de absorvedores de baixo custo para ASAs. **Métodos**: Três configurações de absorvedores (tubo de alumínio, mangueira corrugada de folha de alumínio e placa trapezoidal de aço galvanizado) foram construídas na Universidade de Misan, Maysan, Iraque. O ASA foi testado sob convecção natural e forçada, com ângulos de inclinação de 25°, 30° e 35°. A eficiência térmica foi calculada utilizando a primeira lei da termodinâmica, enquanto a eficiência exergética foi determinada por meio do modelo do fator de Petela. **Resultados**: Sob convecção natural, o absorvedor trapezoidal de aço alcançou o maior incremento de temperatura do ar (~65 °C próximo ao meio-dia solar). O ângulo de inclinação ótimo foi de 30°, proporcionando uma temperatura do ar na saída de aproximadamente 90 °C. Sob convecção forçada, a eficiência térmica atingiu um máximo de 22,9% e a eficiência exergética alcançou 0,14% para o absorvedor trapezoidal, ambos superiores aos das configurações de mangueira de folha de alumínio (21%; 0,13%) e tubo de alumínio (20%; 0,12%). O custo total de fabricação variou entre USD 120 e 150. **Discussão**: A convecção forçada melhorou a transferência de calor ao aumentar o coeficiente convectivo e reduzir a resistência da camada limite térmica, resultando em eficiências superiores tanto pela primeira quanto pela segunda lei da termodinâmica, apesar de um menor incremento de temperatura. As baixas eficiências exergéticas são consistentes com a literatura para sistemas solares térmicos de baixa temperatura e refletem a irreversibilidade inerente à conversão de radiação solar de alta qualidade em calor de baixa qualidade. **Conclusões**: O absorvedor trapezoidal de aço galvanizado, orientado a 30° e operado sob convecção forçada moderada, constitui a configuração de ASA mais eficiente do ponto de vista termodinâmico e mais econômica entre as avaliadas. Os resultados sustentam a viabilidade de ASAs fabricados localmente para aplicações domésticas e agrícolas em regiões rurais e de alta irradiância.

Palavras-chave: *Aquecedor Solar de Ar; Eficiência exergética; Eficiência térmica; Materiais de baixo custo; Absorvedor trapezoidal.*

DOI: 10.52571/PTQ.v23.n52.2026_10_ALI_pgs_126_141.pdf

ABSTRACT

Background: Solar air heaters (SAHs) represent a promising passive solar technology for space heating and drying applications. Despite their potential, the combination of thermal (first-law) and exergy (second-law) performance evaluation for SAHs fabricated from low-cost, locally available materials remains largely unexplored. **Aim:** This study aimed to design, build, and experimentally evaluate three low-cost SAH absorber configurations. **Methods:** Three absorber configurations (i.e., aluminium tube, corrugated aluminium foil hose, and trapezoidal galvanized steel plate) were constructed at the University of Misan, Maysan, Iraq. The SAH was tested under natural and forced convections at tilt angles of 25°, 30°, and 35°. Thermal efficiency was calculated using the first law of thermodynamics, while exergy efficiency was determined using the Petela factor model. **Results:** Under natural convection, the trapezoidal steel absorber achieved the highest air temperature increment (~65 °C near solar noon). The optimal tilt angle was 30°, yielding an outlet air temperature of approximately 90°C. Under forced convection, the trapezoidal absorber achieved thermal efficiency of 22.9% and exergy efficiency of 0.14%, both superior to the aluminium foil hose (21%; 0.13%) and aluminium tube (20%; 0.12%) configurations. Total fabrication cost ranged from USD 120 to 150. **Discussion:** Forced convection improved heat transfer by increasing the convective coefficient and reducing thermal boundary layer resistance, resulting in superior first- and second-law efficiencies despite a lower temperature increment. The low exergy efficiencies are consistent with the literature for low-temperature solar thermal systems and reflect the inherent irreversibility of converting high-grade solar radiation into low-grade heat. **Conclusions:** The trapezoidal galvanized steel absorber, oriented at 30° and operated under moderate forced convection, constitutes the most thermodynamically efficient and cost-effective SAH configuration among those evaluated. The findings support the viability of locally manufactured SAHs for domestic and agricultural applications in rural and high-irradiance regions.

Keywords: *Solar Air Heater; Exergy efficiency; Thermal efficiency; Low-cost materials; Trapezoidal absorber.*

الملخص

الخلفية: تُعدّ سخانات الهواء الشمسية (SAHs) إحدى التقنيات الشمسية السلبية الواعدة في تطبيقات التدفئة وتجفيف المواد. وعلى الرغم من الإمكانات الكبيرة لهذه الأنظمة، فإن الدراسات التي تجمع بين تقييم الأداء الحراري (القانون الأول للديناميكا الحرارية) والأداء الإكسرجي (القانون الثاني) لسخانات الهواء الشمسية المصنَّعة من مواد منخفضة التكلفة ومتوفرة محلياً ما تزال محدودة. **الهدف:** هدفت هذه الدراسة إلى تصميم وتصنيع وتقييم الأداء التجريبي لثلاثة نماذج منخفضة التكلفة لممتصات سخان الهواء الشمسي. **طرائق العمل:** تم تصنيع ثلاث نماذج من الممتصات (أنبوب من الألمنيوم، خرطوم مموج من رقائق الألمنيوم، وصفيحة فولاذية مجلفنة ذات شكل شبه منحرف) في جامعة ميسان، محافظة ميسان، العراق. وتم اختبار سخان الهواء الشمسي في حالتي الحمل الطبيعي والقسري عند زوايا ميل قدرها 25° و30° و35°. حُسبت الكفاءة الحرارية باستخدام القانون الأول للديناميكا الحرارية، بينما حُددت الكفاءة الإكسرجية باستخدام نموذج عامل بيتلا (Petela). **النتائج:** في حالة الحمل الطبيعي، حقق الممتص الفولاذي شبه المنحرف أعلى زيادة في درجة حرارة الهواء (حوالي 65 °م عند ذروة الإشعاع الشمسي). وكانت زاوية الميل المثلى 30°، حيث بلغت درجة حرارة الهواء الخارج نحو 90 °م. أمّا في حالة الحمل القسري، فقد حقق الممتص شبه المنحرف كفاءة حرارية بلغت 22.9% وكفاءة إكسرجية بلغت 0.14%، وهي قيم أعلى من تلك التي حققها خرطوم رقائق الألمنيوم (21%؛ 0.13%) وأنبوب الألمنيوم (20%؛ 0.12%). وتراوحت تكلفة التصنيع الكلية بين 120 و150 دولارًا أمريكيًا. **المناقشة:** أدّى الحمل القسري إلى تحسين انتقال الحرارة من خلال زيادة معامل الحمل الحراري وتقليل مقاومة طبقة الحد الحرارية، مما نتج عنه تحسين الكفاءتين الحرارية والإكسرجية رغم انخفاض مقدار الزيادة في درجة الحرارة. كما أن انخفاض الكفاءة الإكسرجية يتوافق مع ما ورد في الأدبيات الخاصة بالأنظمة الشمسية الحرارية منخفضة الحرارة، ويعكس الطبيعة اللاإنعكاسية لتحويل الإشعاع الشمسي عالي الجودة إلى حرارة منخفضة الجودة. **الاستنتاجات:** يُعدّ الممتص الفولاذي المجلفن ذو الشكل شبه المنحرف، عند زاوية ميل 30° وتشغيله تحت حمل قسري معتدل، التكوين الأكثر كفاءةً من الناحية الديناميكية الحرارية والأكثر جدوى اقتصادية بين النماذج المدروسة. وتدعم هذه النتائج جدوى استخدام سخانات الهواء الشمسية المصنّعة محليًا في التطبيقات المنزلية والزراعية في المناطق الريفية والمناطق ذات الإشعاع الشمسي العالي.

الكلمات المفتاحية :سخان الهواء الشمسي؛ الكفاءة الإكسرجية؛ الكفاءة الحرارية؛ مواد منخفضة التكلفة؛ ممتص شبه منحرف.

1. INTRODUCTION:

Since humans settled on Earth, they have found that the sun is the most important source of warmth and energy for life, and for survival, they have continued to travel to the sunniest places. Over the centuries, many architectural alterations were adopted to capture the heat transmitted by the sun, especially in cold climates (Saxena *et al*., 2015). Nowadays, solar energy is not limited to heating; it is also used to generate electricity. Many applications, such as heating, cooling, food cooking, battery charging, and lighting, were integrated with solar energy in buildings (Sayigh, 2012). The applications of investing in solar energy are generally divided into two sectors (i.e., thermal and non-thermal applications) and solar energy conversion. The thermal applications included water and space heating, cooling and refrigeration, water purification, food cooking, and product drying (AMORIM *et al*., 2020; Close, 1963; Indora *et al*., 2018; Kalogirou S. A., 2004; RABAT *et al*., 2018; El Khadraoui *et al*., 2016). Non-thermal applications, on the other hand, can include electricity generation, battery charging,

building lighting, transportation, irrigation, and communication and navigation aids (Ollas *et al*., 2023; Bartłomiejczyk, 2018; El-Faouri *et al*., 2016; Gibson & Kelly, 2009; Kanna *et al*., 2020; Siddikov *et al*., 2021).

A solar air heater (SAH) is one of the most attractive passive solar methods for converting incident solar radiation into air heating. SAHs are an increasingly important technology in renewable energy, providing a sustainable and efficient means of space heating. The heat captured using SAHs can not only be used for residential, commercial, and industrial building air conditioning, but also for drying crops and clothes, and for heating animal pens during cold winters. This technology offers significant environmental benefits by reducing reliance on fossil fuels and decreasing greenhouse gas emissions. Additionally, SAHs are relatively low-cost and require minimal maintenance, making them accessible and practical for widespread use.

Research shows that solar air heaters (SAH) can be classified by collector geometry, construction material, airflow configuration, and heat transfer enhancement practices. One important parameter, amongst others, is the construction material used, which will strongly affect both the economic benefits and the thermal performance of an SAH system. Lightweight, low-cost materials such as corrugated steel sheets, aluminium plates, or polymer-based components have been used in practice because they are widely available and easy to make. Passive solar heat storage systems were used in buildings as early as the end of the 1800's, using simple glazing on large amounts of glass to capture the sun's heat and improve the indoor environment's thermal conditions. Modern SAH systems have built on this history with enhanced absorber geometry, optimised airflow designs, and high-performance materials which work together to create systems with superior thermal efficiency while being produced for very low costs (Ahmadi *et al*., 2021; Hegde *et al*., 2023; Kalair *et al*., 2022, PORTELA *et al*., 2020).

In the common design, there were two layers of glazing with two vertical chambers separated by a thin transparent foil, and a top layer of glazing that allows natural convection airflow. The chambers heated up as the sun hit the glazing, with the chamber next to the wall heating up first. The transparency of common materials limited the usable materials for construction. Other design types involved glazing and a range of black-absorbing materials, with air convection behind the heated surface. Different materials, such as Aluminium, twin-pack, dark metal glazing, wooden, and black mesh, were used as absorbers. (Arıcı *et al*., 2020; Piffer *et al*., 2022). Some designs used fans to assist air flow, while others relied on natural convection, often determined by stack height on the unglazed side (Song *et al*., 2022; Fan *et al*., 2022; Stafford *et al*., 2021). A suitably selected material can be highly efficient and be called a passive system, since it does not require a fan to displace the air to be heated (Ghritlahre *et al*., 2022).

The availability and cost of building materials significantly influence the feasibility and sustainability of solar thermal systems in developing areas. Using cheap, locally available materials to build SAHs lowers capital costs and enables systems to be built, run, and maintained without relying on imported parts or specialized manufacturing resources. This method helped communities become more self-sufficient and made it easier for more people to use renewable heating technologies, especially in rural and low-income areas (Chandran *et al*., 2024). In addition, using common materials such as aluminium sheets, galvanized steel plates, and flexible foil ducts can reduce the manufacturing costs while having high thermal performance (Saxena *et al*., 2015). As a result, low-cost, cost-effective SAHs made from locally sourced materials are an essential strategy for enhancing renewable energy adoption and reducing dependence on fossil fuels (Kalogirou, 2004). Although solar energy is significantly available in southern Iraq, the utilisation of solar thermal technology is limited by economic barriers and insufficient industrial infrastructure. The thermal efficiency of SAHs has been investigated extensively over the last decade; however, less effort has been devoted to exergy efficiency, which assesses the quality of energy (Albdoor *et al*., 2024; Kalaiarasi *et al*., 2016).

While many efforts have been made to investigate the performance improvement of SAHs, there has been a notable lack of research on low-cost prototypes fabricated from locally available materials. In this study, a prototype of SAH made from low-cost, readily available materials with high thermal performance was developed in a typical region with high solar irradiation. In this SAH, three absorber configurations (i.e., aluminium tubes, aluminium foil hoses, and trapezoidal steel plates) coated with black matte were tested under natural and forced convection at different tilt angles. This research also provides practical guidance for

optimal design and implementation by analysing outlet air temperature, thermal and exergy efficiencies, and operational behaviour across various configurations.

1.1. Aims

- To design and fabricate a solar air heater using low-cost, locally available materials.
- To experimentally compare the performance of three absorber geometries under identical operating conditions.
- To evaluate the influence of tilt angle and airflow mode (natural and forced convection) on temperature rise and thermal efficiency.
- To perform a second-law (exergy) analysis to assess energy quality and system irreversibility.
- To assess the economic feasibility of locally manufactured SAH systems for practical deployment.

2. MATERIALS AND METHODS:

2.1. Location and climatic conditions

The experiments were conducted in Maysan, Iraq (31.9°N, 47.1°E), where the average solar irradiance at noon during the test season is between 750 and 900 W/m². The climate has a lot of direct sunlight and little humidity, making it a good place for solar air heating.

2.2. Solar air heater construction

The SAH was built as a flat-plate collector, as shown in Figure 1. The collector box was made with an L-shaped steel frame, which made it strong and stable with respect to temperature. The overall area of the solar collector was 1.275 m², and 8 mm plywood covered the inner side walls, and a 10 mm fiberglass insulation blanket covered the parts not exposed to the outside. The glazing cover was a 4 mm-thick sheet of clear glass, chosen for its ability to let a lot of light through and withstand bad weather. The air inlet was at the bottom of the collector, and the outlet was at the top. This made it easy for both natural and forced air to move through the collector.

2.3 Configurations of the absorber plate

Three absorber configurations were designed and evaluated, each coated with black matte paint Figure 2.

- **Aluminium tube absorber:**

Ten aluminium tubes, length of 1.5 m, diameter of 7.62 cm, and overall solar captured area of 1.05 m² arranged vertically. Tubes create parallel air passages, allowing convective heat transfer.

- **Aluminium foil hose absorber:**

Six flexible corrugated aluminium hoses arranged vertically, with a diameter of $10.16\ cm$, and the dimensions of the exposed surface were (150×70 cm). The corrugated texture increases surface turbulence, which enhances heat transfer.

- **Trapezoidal steel plate absorber:**

Single sheet of corrugated trapezoidal steel, the dimensions of the exposed surface were (150×70 cm), thickness of 0.7mm. The corrugation increases effective surface area and enhances air surface contact.

2.4 Operating modes

The SAH was examined under two scenarios:

- **Natural convection:** No fan assistance; airflow driven by natural convection.
- **Forced convection:** Air is supplied by a fan at the outlet side, operating at 220-240 V, 50/60 Hz, with a rotation speed of 2250 rpm and an electric power of 19 W. A multi-level voltage regulator was used to control the fan speed and thus adjust the airflow rate based on the experimental conditions. The forced mode might increase airflow rate, reduce air residence time, and improve convective heat transfer.

2.5 Instrumentation and data collection

All tests were performed when the sky was clear, so cloud shading wouldn't significantly alter the measurements. Data were collected every hour from 7:20 to 16:20, when solar radiation was at its highest. K-type thermocouples were placed at the air entry and exit points to ensure that the bulk air temperature changes were accurately represented. A digital thermometer was used to monitor the ambient temperature, and the wind speed was checked periodically to assess its effect on heat loss by convection. The SAH was tested at three different angles (i.e., 25°, 30°, 35°) to see how the angle of tilt affected the system's thermal behavior Figure 3.

2.6 Performance evaluation

The model developed by Ref. (Chamoli, 2013) for evaluating SAH performance was based on useful heat gain, thermal efficiency, and the effects of airflow regime and absorber configuration on the temperature rise. The assessment was predicated on the recorded inlet and outlet air temperatures, solar irradiance, and mass flow rate. The useful heat gain is the amount of thermal energy that flows from the absorber to the air flowing through it. It is calculated as Equation 1:

$$Q_u = \dot{m}.C_p\,(T_{out} - T_{in}) \qquad (Eq.1)$$

where $\dot{m}$ is the mass flow rate of air (kg/s), $C_p$is the specific heat capacity of air, and $T_{out} - T_{in}$is the temperature rise of the air as it passes through the collector. In forced convection mode, the mass flow rate was obtained from measured airflow velocity using Equation 2:

$$\dot{m} = \rho V A_d \qquad (Eq.2)$$

where ρ is the air density, V is the air velocity (m/s), and $A_d$is the cross-sectional area of the air duct. Using a digital anemometer, airflow velocity within the collector was measured directly at the outlet of the air channel. The instrument has an accuracy of ±0.03 m/s (0-10m/s) with the ability to make this measurement in the middle of the outlet duct. Each measurement was recorded at every experimental time interval.

The instantaneous thermal efficiency of the collector was then calculated using Equation 3:

$$\eta_{th} = \frac{Q_u}{I.A_c} \qquad (Eq.3)$$

where I is the measured plane-of-array solar irradiance (W/m²) and A_c is the collector's exposed area. This efficiency reflects the proportion of incident solar energy that is successfully converted into useful heating of the air stream.

To assess the impact of airflow rate on heat transfer, a thermal performance analysis was conducted under both natural and forced convection conditions. In forced convection, higher airflow velocity increases the convective heat transfer coefficient, enhancing heat removal from the absorber surface and leading to higher thermal efficiency even when the outlet air temperature rise is smaller. In contrast, natural convection typically produces a higher temperature rise but a lower mass flow rate, resulting in lower overall heat gain.

2.7 Exergy Analysis

To assess the quality of the collected solar energy, the exergy (second-law) efficiency was computed for each timestamp and operating mode (Chamoli, 2013; Petela, 2003). The useful exergy rate of the heated airstream, neglecting pressure effects and assuming ideal-gas behaviour for air, is given by Equation 4:

$$\dot{E}_u = \dot{m}\,C_p[(T_{out} - T_{in}) - T_a\,ln\left(\frac{T_{out}}{T_{in}}\right) \qquad (Eq.4)$$

where $\dot{m}$ is the air mass flow rate, T_{in} and T_{out} are the inlet and outlet air temperatures (K), and T_a is the ambient. Equation (5) presented the **solar exergy input** to the collector aperture. A_c that was estimated with the Petela factor ϕ that is presented in Equation (6).

$$\dot{E}_\odot = I_{POA} A_c \emptyset \qquad (Eq.5)$$

$$\emptyset = 1 - \frac{4}{3}\frac{\mathrm{T_a}}{\mathrm{T_\odot}} + \frac{1}{3}\left(\frac{\mathrm{T_a}}{\mathrm{T_\odot}}\right)^4 \qquad (Eq.6)$$

with I_{POA} the plane-of-array irradiance on the collector tilt.

The exergy (second-law) efficiency is given by Equation (7):

$$\psi = \frac{\dot{\mathrm{E}}_\mathrm{u}}{\dot{\mathrm{E}}_\odot} \qquad (Eq.7)$$

and the exergy destruction rate quantifies irreversibility: $\dot{E}_{dest} = \dot{E}_\odot - \dot{E}_u$

The overall parameters used in the analytical evaluation is presented in Table 1.

2.8 Uncertainty analysis

The uncertainty associated with the measured variables propagates into the calculated thermal and exergy efficiencies. The main measured parameters include air temperature and air velocity. Each measuring instrument introduces measurement error, which contributes to the overall uncertainty of the calculated results.

The uncertainties in the calculated exergy and thermal efficiencies were estimated using the basic root-sum-square (RSS) method. If a parameter F is a function of a series of measured independent variables x_i, the relative uncertainty δRF for the F can be acquired according to

Equation 8 (Yang *et al*., 2015):

$$\delta RF = \frac{\sqrt{\sum_1^n \left(\frac{\partial F_i}{x_i}.\delta x_i\right)^2}}{F} \qquad (Eq.\ 8)$$

where:

- Thermocouple temperature measurement: ±0.5 °C.
- Air velocity measurement: ±0.03 m/s.

The combined uncertainty of the thermal efficiency was estimated at ±0.8% to ±1.8%, while the uncertainty of the exergy efficiency was ±0.005% to ±0.015%.

These uncertainty levels are within the acceptable range for experimental solar thermal system studies reported in the literature.

2.9 Cost-effective material selection

The material selection for the solar air heater prototypes was based on optimizing thermodynamic performance and ensuring economic viability for potential widespread deployment in the local Iraqi market. Aluminium tubes, corrugated aluminium foil hoses, and trapezoidal galvanized steel sheets were selected based on their local market availability, low cost, ease of fabrication, and favourable thermal properties. The overall prices of components used in the design and construction of SAH were presented in Table 2. The total fabrication cost for the solar collector ranged from approximately $120 to $150, depending on the specific absorber configuration. Aluminium was selected because of its high thermal conductivity and low weight. The trapezoidal galvanized steel, on the other hand, offers structural rigidity and a geometrically augmented heat transfer surface area, achieved without specialized manufacturing processes. All absorber surfaces were coated with a low-cost matte-black paint to enhance solar energy absorption. In addition, the use of locally sourced materials facilitates easier maintenance, enhances local repairability, and ensures long-term sustainability, all of which are considered critical factors for adoption in rural and low-income communities.

3. RESULTS AND DISCUSSION:

3.1. Comparison of air temperature increase across absorber geometries

Figure 4 shows the hourly temperature increments, expressed as the difference between the outlet and inlet air temperatures, for three absorber geometries under natural convection. The configurations evaluated were the aluminium tube, aluminium foil hose, and trapezoidal steel plate. The temperature increment increases gradually from early morning (around 7:20 AM) as solar irradiance intensifies, reaches its peak between 11:20 AM and 12:40 PM, and gradually declines in the afternoon due to reduced solar flux and accumulated thermal losses. Under natural convection, the trapezoidal steel absorber achieved the highest temperature increment, recording around 65 °C near noon. The aluminium foil hose exhibited intermediate performance with a temperature increment ranging between (55–60 °C), while the aluminium tube absorber displayed the lowest increment (below 50 °C). The temperature increment in the trapezoidal design was attributed to its corrugated surface geometry, which increases the effective heat-transfer area and induces mild turbulence, enhancing air mixing. The other two absorbers, being smoother and less conductive, developed weaker buoyancy-driven airflow and lower air-temperature elevation.

Under forced convection, the overall temperature increments as shown in Figure 5 were smaller than those of natural convection, which are 30 °C for the trapezoidal steel plate, 26 °C of aluminium foil hose, and 20 °C of aluminium tube; because the fan-driven flow (1.2 m/s) increased the flow rate of mass and reduced the residence time of air inside the duct.

3.2 Effect of tilt angle on temperature distribution under natural convection

Figure 6 presents the variation in air temperature over time for the trapezoidal steel plate absorber operating under natural convection at three tilt angles (25°, 30°, and 35°), along with the inlet-air temperature for reference. A clear diurnal pattern is observed across all tilt settings: the outlet temperature increases gradually from the morning hours as solar irradiance rises, reaches a maximum between 11:20 AM and 12:40 PM, and then decreases toward the late afternoon as solar irradiance declines. The results demonstrate a distinct influence of the collector inclination on thermal performance. The collector tilted at 30° achieved the highest leaving air temperature, approximately 90 °C, at 11:20 AM and 12:20 PM. The 25° tilt configuration exhibited slightly lower maximum temperatures, while the 35° tilt

recorded a peak that was similar, though marginally lower. This indicates that the 30° inclination provides the optimum orientation for maximizing solar radiation absorption and heat transfer to the air. At smaller angles (25°), part of the incident solar energy is reflected due to the shallower orientation relative to the solar beam, reducing effective insolation during morning and afternoon periods. Conversely, at higher tilt (35°), the collector receives less direct radiation near noon when the solar altitude is highest, slightly diminishing thermal gain despite improved morning and evening collection. Across all tilt angles, the trapezoidal absorber maintained a strong temperature gradient due to its corrugated design and high thermal conductivity, which enhanced buoyancy-driven air circulation even without forced flow.

3.3 Thermal efficiency under natural and forced convection

Figure 7. illustrates the diurnal variation of thermal efficiency for the solar air heater operating under natural and forced convection conditions. Efficiency increased progressively from early morning as solar irradiance intensified, reached its maximum around solar noon (11:20 AM–12:40 PM), and then gradually declined as solar radiation decreased in the afternoon. The collector operating under forced convection clearly outperformed the natural-flow configuration throughout the day. At midday, the efficiency reached a peak value of approximately 22.9 % for the forced-flow system, compared with 15.5 % for natural convection. The superior performance under forced flow is primarily attributed to the higher air mass flow rate, which enhanced the convective heat transfer coefficient, minimized the thermal boundary layer on the absorber surface, and reduced temperature stratification inside the duct. Although the outlet-air temperature difference was smaller under forced operation, the overall useful heat gain was significantly higher due to the higher rate of energy transport. In contrast, the natural-convection mode, driven solely by buoyancy forces, exhibited lower heat-extraction efficiency and greater temperature nonuniformity along the flow path.

3.4 Comparative performance of absorber geometries

Figure 8 compares the thermal and exergy efficiencies of the three absorber geometries under forced convection. All configurations show a strong daily trend, with efficiencies steadily rising from morning hours as solar irradiance increases, peaking around 12:20 PM and slowly falling toward late afternoon. The trapezoidal absorber achieves the highest thermal efficiency, peaking at approximately 23%, followed by the aluminium foil hose at 21% and the aluminium tube at 20%. The trapezoidal shape has better heat transfer properties because it provides a larger effective surface area and generates stronger airflow turbulence, thereby improving convective heat transfer. A corresponding trend is evident in the exergy efficiency, which quantifies the quality and useful work potential of the thermal energy delivered.

Even though the absolute exergy values are usually low for a low-temperature solar thermal system, they still follow the same performance order as the thermal efficiency, indicating that geometry affects performance. The trapezoidal absorber achieved the highest exergy efficiency at approximately 0.14%, followed by the foil hose of 0.13% and the aluminium tube of 0.12%. The higher air velocity in the SAH increased the heat transfer coefficient, resulting in higher thermal efficiency regardless of the lower temperature increment. A comparison of the two flow regimes reveals a fundamental thermodynamic trade-off between temperature elevation and heat transfer rate. While natural convection yields a higher outlet temperature, its useful heat gain is constrained by a limited air mass flow rate. Conversely, forced convection achieves a lower temperature increment but attains a higher overall heat collection efficiency due to its higher volumetric flow rate. Across both operational modes, the trapezoidal absorber demonstrated consistent performance superiority over the foil and tubular designs, underscoring the pronounced influence of absorber geometry and material thermal conductivity on the collector's temperature field. The observed correlation between thermal and exergy efficiencies suggests that geometric improvements to the absorber not only enhance useful heat gain but also reduce thermodynamic irreversibility, including non-uniform temperature distribution and entropy generation.

3.5 Exergy performance and irreversibility trends

Figure 9 illustrates the behaviour of exergy efficiency and normalized exergy destruction for both natural and forced convection modes. The exergy efficiency increases gradually from early morning, reaching a maximum near solar noon, and subsequently decreases as solar irradiation weakens. Forced convection consistently produces higher exergy efficiency, reaching up to 0.14%, compared to natural convection, which peaks at 0.09%. This

improvement is attributed to the enhanced air mass flow rate under forced operation, which reduces temperature gradients within the collector and promotes more effective utilization of the absorbed solar exergy. The lower panel shows the corresponding trend of normalized exergy destruction, which is inversely related to exergy efficiency. Natural convection exhibits significantly higher exergy destruction during morning and afternoon periods due to strong temperature non-uniformity and limited internal heat transfer.

In contrast, forced convection suppresses irreversibility during peak solar hours, with destruction levels dropping to their lowest values around noon, when flow-induced mixing is strongest. The alignment of minimum exergy destruction with maximum exergy efficiency confirms the strong thermodynamic advantage of assisted airflow operation. Overall, the figure emphasizes that forced convection results in a more thermodynamically reversible process, reducing entropy generation and improving the quality of the useful energy delivered by the system. These results align with previously reported findings in the literature, where exergy efficiency of SAHs improves under higher mass-flow rates due to enhanced convective heat transfer and reduced internal irreversibility. The trends shown reaffirm that for hot, high-irradiance climates such as Maysan, Iraq, a fan-assisted configuration is markedly superior for improving system sustainability and second-law performance.

3.6 Energy–exergy correlation and design implications

Figure 10 illustrates the relationship between thermal and exergy efficiencies for a solar air heater with a trapezoidal absorber operating under forced convection. A clear positive correlation is observed, indicating that as the collector extracts more useful thermal energy from incident solar radiation, the fraction of that energy converted into available (high-grade) work also increases. The linear regression trend confirms that second-law performance improves proportionally with first-law efficiency, highlighting the importance of enhancing convective heat transfer and reducing internal temperature gradients. While exergy efficiencies remain significantly lower than thermal efficiencies, as expected for low-temperature solar systems, the upward trend demonstrates that design features that promote uniform heating, improved mixing, and reduced thermal resistance (such as the trapezoidal geometry) simultaneously reduce irreversibility and entropy production. This reinforces the conclusion that optimizing absorber geometry and airflow not only increases heat gain but also enhances the thermodynamic quality of the energy delivered by the solar air heater.

4. CONCLUSIONS:

This work conducted a performance evaluation of a low-cost solar air heater (SAH) using thermal and exergy efficiencies. The materials used to construct SAHs were locally available and economically viable. Three different configuration absorbers (i.e., parallel aluminium tubes, a corrugated aluminium foil hose, and a trapezoidal galvanized steel plate) were experimentally examined under natural and forced convection regimes. The influence of tilt angles on the SAH performance was also investigated under (25°, 30°, and 35°). The results showed that the trapezoidal steel absorber performed better than other configurations, achieving the highest outlet temperatures and the greatest thermal and exergy efficiencies. The most stable operation and higher solar energy capture were achieved at a SAH tilt angle of 30°. The results also showed that natural convection had higher outlet temperatures than forced convection.

Meanwhile, under forced convection, the thermal and exergy efficiencies were 22.9% and 0.14%, respectively, for a 30° tilt angle and a trapezoidal galvanized steel plate configuration. Exergy analysis indicated that, while characteristically low for a low-temperature thermal system, it improved under forced convection, reaching a peak value of 0.14% for the trapezoidal absorber at a 30° tilt angle. This enhancement is attributed to reduced thermal gradients and the associated irreversibility within the collector. An economic assessment confirmed the cost-effectiveness of this approach; the complete experimental apparatus, including all absorber variants, glazing, insulation, and instrumentation, was fabricated for approximately 120 and 150 USD. This underscores the potential for localized manufacturing and deployment in rural or low-income settings. In conclusion, the results indicate that a simple, economically fabricated SAH incorporating a trapezoidal steel absorber at a 30° tilt and operated under moderate forced convection constitutes a practical and efficient heating solution for domestic and agricultural applications in regions of high solar insolation.

5. DECLARATIONS

5.1. Study Limitations

Although the present study provides valuable insights into the thermal and exergy performance of a low-cost solar air heater constructed from locally available materials, several limitations should be acknowledged.

Methodological limitations: The experimental investigation was conducted under outdoor environmental conditions, where solar irradiance, ambient temperature, and wind speed naturally fluctuate throughout the day. Although efforts were made to measure accurately and average over a set period to reduce variability, environmental factors may still have affected how much heat the thermometer measured and how efficiently the solar collector operates. In addition, the research study focused mainly on steady-state conditions and did not examine how the solar collector operated under changing conditions over time.

Sample size and experimental replication: The experiments were conducted over a limited number of days due to timing and conditions. With a larger sample size, we could evaluate how the systems operate more fully. If we did more repetitions of the tests, we could statistically validate the outcomes.

Resource and Equipment Limitations: The experiments were set up using commercially available sensors and tools, all of which were calibrated to measure accurately. Due to this, the accuracy of the readings from the thermocouples, solar meters, and anemometers introduces uncertainty that may impact the calculated thermal and exergy efficiencies. The use of higher-grade instruments could improve precision in future studies.

Generalizability limitations: The experimental testing was conducted in Maysan, Iraq, where the climate is characterized by high solar radiation and high ambient temperatures. The results of this study may differ if the same system were applied in different climatic regions, such as cold climates or areas with low solar irradiance. Therefore, the results reported in this study should be viewed only in the context of a similar type of climate.

Scope limitations: In this investigation, we compared three different absorber geometries in a single-pass solar air heater configuration. No other design configurations (e.g., multi-pass air channels, absorbers with selective coatings, thermal energy storage integration, or variations in air flow) were considered. Our evaluation was limited to thermal and exergy performance; we did not consider long-term durability or an economic life-cycle evaluation of the solar air heater, as these topics were beyond the scope of this research.

5.2. Acknowledgments

The College of Engineering at Misan University in Misan is thanked for providing technical assistance and the lab equipment needed to conduct this research experiment. The authors also thank all those who provided technical assistance with equipment setup and data collection, including coworkers and other staff members.

5.3. Funding Sources

The authors funded this research.

In accordance with Periódico Tchê Química's ethical guidelines, which prohibit donations from authors with manuscripts under review (even when research funds are available), or in cases of author financial constraints, publication costs were fully absorbed by the journal under our Platinum Open Access policy, with support from Araucária Scientific Association (https://acaria.org/). This policy ensures complete independence between the editorial process and any financial aspects, reinforcing our commitment to scientific integrity and equitable knowledge dissemination.

5.4. Conflicts of Interest

The authors declare no conflicts of interest.

5.5. Data Availability

All data presented in this study are available in the manuscript tables and figures. Raw data are available upon request from the corresponding author.

5.6. Author Contributions

Ali Al-Jubainawi: CD, DAI, MW, FA. Mahmood S. Mahmood: DC, DAI, CR. Mohammed Abbas: DC, DAI. Abbas Bleash: CR, MW. Mustafa Ajeal: CR, FA.

5.7. AI and Computational Tools Declaration

The authors declare that no generative artificial intelligence tools or computational language models were used in the conception, design, execution, data collection, data analysis, interpretation, manuscript writing, or any other aspect of this research or manuscript preparation.

5.8. Research Integrity Declaration

The authors confirm that this work contains no previously published work. The authors have maintained research integrity in all aspects of this study, including no data fabrication or manipulation and no selective reporting of results. All methods of this study were conducted ethically, and all results have been reported as accurately and transparently as possible.

5.9. Originality & Plagiarism Statement

The authors declare this manuscript is authentic and that this work has not been published nor submitted for publication elsewhere. The manuscript does not contain any plagiarized material, and all sources are appropriately credited. The authors had their manuscript screened with Turnitin to assess originality before submission. The Turnitin software reported a similarity index of 9%, indicating that this manuscript falls within the acceptable range for academic publication. All words, figures, and data within the manuscript meet or exceed the standards of academic integrity through proper referencing.

5.10. Originality Declarations

- Original Work: This manuscript is original work not previously published or under review elsewhere.
- No Unattributed Copying: No text was copied from other sources without proper citation and quotation marks.
- All Sources Properly Cited: All sources are properly cited in APA format.
- Not Submitted Elsewhere: This manuscript is not currently being considered for publication elsewhere.

5.10. Open Access License

6. REFERENCES:

1. Ahmadi, A., Ehyaei, M. A., Doustgani, A., Assad, M. E. H., Hmida, A., Jamali, D. H., & Razmjoo, A. (2021). Recent residential applications of low-temperature solar collector. Journal of Cleaner Production, 279, 123549. Retrieved from: https://doi.org/10.1016/j.jclepro.2020.123549.
2. Albdoor, A. K., Obaid, Z. A. H., Kamel, M. S., & Azzawi, I. D. (2024). Energy, exergy, economic and environmental analysis of a solar air heater integrated with double triangular fins: Experimental investigation. International Journal of Thermofluids, 24, 100979. Retrieved from: https://doi.org/10.1016/j.ijft.2024.100979.
3. AMORIM, N. J. P., LIMA, R., ROCHA, P., MARINHO, F., & SILVA, M. (2020). Experimental analysis of a solar heat system using hybrid silver nanofluid and titanium dioxide. PERIODICO TCHE QUIMICA, 17(34), 448-458. Retrieved from: DOI: 10.52571/PTQ.v17.n34.2020.472_P34_pgs_448_458.pdf.
4. Arıcı, M., Tükel, M., Yıldız, Ç., Li, D., & Karabay, H. (2020). Is the thermal transmittance of air-filled inclined multi-glazing windows similar to that of vertical ones?. Energy and Buildings, 229, 110515. Retrieved from: https://doi.org/10.1016/j.enbuild.2020.110515
5. Bartłomiejczyk, M. (2018). Potential application of solar energy systems for electrified urban transportation systems. Energies, 11(4), 954. Retrieved from: https://doi.org/10.3390/en11040954.
6. Chamoli, S. (2013). Exergy analysis of a

flat plate solar collector. Journal of Energy in Southern Africa, 24(3), 08-13. Retrieved from: https://doi.org/10.3390/e16052549.
7. Chandran, B., Oh, J.-K., Lee, S.-W., Um, D.-Y., Kim, S.-U., Veeramuthu, V., Park, J.-S., Han, S., Lee, C.-R., & Ra, Y.-H. (2024). Solar-driven sustainability: III–V semiconductor for green energy production technologies. Nano-Micro Letters, 16(1), 244. Retrieved from: https://doi.org/10.1007/s40820-024-01412-6.
8. Close, D. J. (1963). Solar air heaters for low and moderate temperature applications. Solar energy, 7(3), 117-124. Retrieved from: https://doi.org/10.1016/0038-092X(63)90037-9
9. El-Faouri, F. S., Sharaiha, M., Bargouth, D., & Faza, A. (2016). A smart street lighting system using solar energy. 2016 IEEE PES Innovative Smart Grid Technologies Conference Europe (ISGT-Europe), Retrieved from: https://doi.org/10.1109/ISGTEurope.2016.7856255.
10. El Khadraoui, A., Bouadila, S., Kooli, S., Guizani, A., & Farhat, A. (2016). Solar air heater with phase change material: An energy analysis and a comparative study. Applied Thermal Engineering, 107, 1057-1064. https://doi.org/10.1016/j.applthermaleng.2016.07.004.
11. Fan, M., Fu, Z., Wang, J., Wang, Z., Suo, H., Kong, X., & Li, H. (2022). A review of different ventilation modes on thermal comfort, air quality and virus spread control. Building and Environment, 212, 108831. Retrieved from: https://doi.org/10.1016/j.buildenv.2022.108831.
12. Ghritlahre, H. K., Verma, M., Parihar, J. S., Mondloe, D. S., & Agrawal, S. (2022). A detailed review of various types of solar air heaters performance. Solar energy, 237, 173-195. Retrieved from: https://doi.org/10.1016/j.solener.2022.03.042
13. Gibson, T. L., & Kelly, N. A. (2009, September). Solar photovoltaic charging of lithium-ion batteries. In 2009 IEEE Vehicle Power and Propulsion Conference (pp. 310-316). IEEE. Retrieved from: DOI: 10.1109/VPPC.2009.5289834
14. Hegde, A. K., Pai, R., & Karanth, K. V. (2023). Performance augmentation of solar air heaters: a comprehensive analysis. Solar Energy, 253, 527-553. Retrieved from: https://doi.org/10.1016/j.solener.2023.01.031.
15. Indora, S., & Kandpal, T. C. (2018). Institutional cooking with solar energy: A review. Renewable and Sustainable Energy Reviews, 84, 131-154. Retrieved from: https://doi.org/10.1016/j.solener.2023.01.031.
16. Kalaiarasi, G., Velraj, R., & Swami, M. V. (2016). Experimental energy and exergy analysis of a flat plate solar air heater with a new design of integrated sensible heat storage. Energy, 111, 609-619. Retrieved from: https://doi.org/10.1016/j.rser.2017.12.001.
17. Kalair, A. R., Seyedmahmoudian, M., Saleem, M. S., Abas, N., Rauf, S., & Stojcevski, A. (2022). A comparative thermal performance assessment of various solar collectors for domestic water heating. International Journal of Photoenergy, 2022(1), 9536772. Retrieved from: https://doi.org/10.1155/2022/9536772
18. Kalogirou, S. A. (2004). Solar thermal collectors and applications. Progress in energy and combustion science, 30(3), 231-295. Retrieved from: https://doi.org/10.1016/j.pecs.2004.02.001.
19. Kanna, R. R., Baranidharan, M., Raja Singh, R., & Indragandhi, V. (2020, September). Solar energy application in Indian irrigation system. In IOP Conference Series: Materials Science and Engineering (Vol. 937, No. 1, p. 012016). IOP Publishing. Retrieved from: DOI 10.1088/1757-899X/937/1/012016
20. Petela, R. (2003). Exergy of undiluted thermal radiation. Solar energy, 74(6), 469-488. Retrieved from: https://doi.org/10.1016/S0038-092X(03)00226-3.
21. Piffer, Y., Jonsson, J. C., Güths, S., Machado, R. M. S., & Lamberts, R. (2022). Development and validation of an optical model for water-based windows with clear glazing: A parametric performance assessment. Building and Environment, 209, 108635. Retrieved from:

https://doi.org/10.1016/j.buildenv.2021.108635.
22. Ollas, P., Sigarchian, S. G., Alfredsson, H., Leijon, J., Döhler, J. S., Aalhuizen, C., ... & Thomas, K. (2023). Evaluating the role of solar photovoltaic and battery storage in supporting electric aviation and vehicle infrastructure at Visby Airport. Applied Energy, 352, 121946. Retrieved from: https://doi.org/10.1016/j.apenergy.2023.121946.
23. PORTELA, L., Almeida, A. F. L., BARBOSA, E., Cezar, K. L., & Oliveira, P. A. (2020). Energy analysis and performance of a parabolic cylindrical solar collector aided by solar tracking system. PERIODICO TCHE QUIMICA, 17(34), 53-61. Retrieved from: DOI: 10.52571/PTQ.v17.n34.2020.71_P34_pgs_53_61.pdf.
24. RABAT, O. Z., ABSAMETOV, D., KUNELBAYEV, M. M., HASANOV, E. L., MYKHALEVSKIY, D. V., ABDRASHITOVA, R. N., & SALNIKOVA, Y. I. (2018). CÁLCULO DE DESEMPENHO DA UNIDADE DE AQUECIMENTO DE ÁGUA SOLAR EM UM POSTO DE GASOLINA. Periódico Tchê Química, 15(30). Retrieved from: DOI:10.52571/PTQ.v15.n30.2018.593_Periodico30_pgs_589_598.pdf
25. Saxena, A., & El-Sebaii, A. A. (2015). A thermodynamic review of solar air heaters. Renewable and Sustainable Energy Reviews, 43, 863-890. Retrieved from: https://doi.org/10.1016/j.rser.2014.11.059
26. Sayigh, A. A. M. (Ed.). (2012). Solar energy application in buildings. Elsevier. DOI:10.1016/B978-0-12-620860-3.X5001-2.
27. Siddikov, I., Khasanov, D., Khujamatov, H., & Reypnazarov, E. (2021, November). Communication architecture of solar energy monitoring systems for telecommunication objects. In 2021 International Conference on Information Science and Communications Technologies (ICISCT) (pp. 01-05). IEEE. Retrieved from: https://doi.org/10.1109/ICISCT52966.2021.9670354
28. Song, W., Zhang, Z., Chen, Z., Wang, F., & Yang, B. (2022). Thermal comfort and energy performance of personal comfort systems (PCS): A systematic review and meta-analysis. Energy and Buildings, 256, 111747. Retrieved from: https://doi.org/10.1016/j.apenergy.2023.121946.
29. Stafford, J., & Xu, C. (2021). Cooling in poor air quality environments—Impact of fan operation on particle deposition. IEEE Transactions on Components, Packaging and Manufacturing Technology, 11(8), 1206-1213. Retrieved from: https://doi.org/10.1109/TCPMT.2021.3084047.
30. Yang, W., Sun, L., & Chen, Y. (2015). Experimental investigations of the performance of a solar-ground source heat pump system operated in heating modes. Energy and Buildings, 89, 97-111. Retrieved from: https://doi.org/10.1016/j.enbuild.2014.12.027.

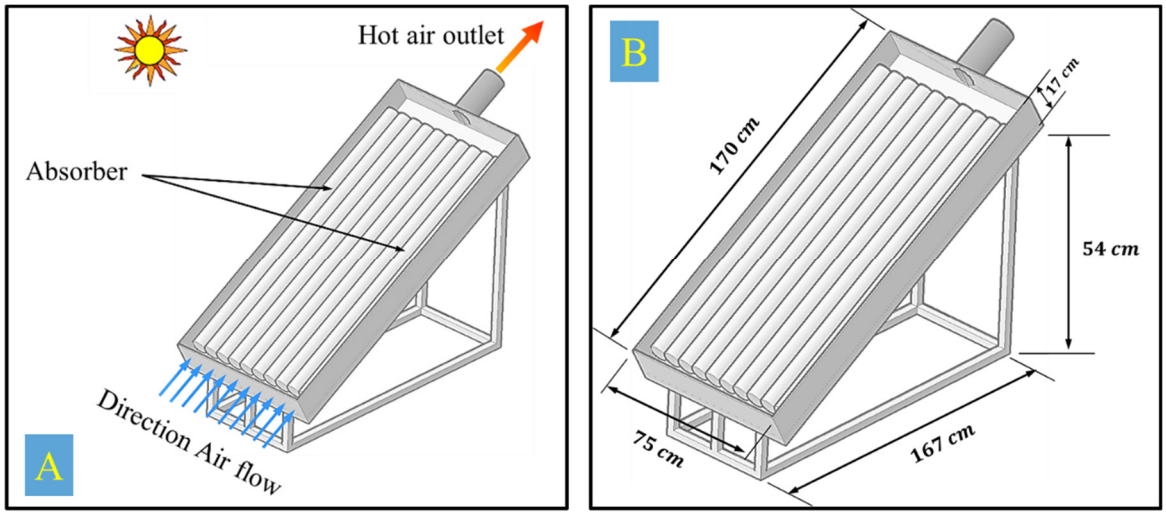

***Figure 1**. Illustration of the dimension and configuration of SAH.*

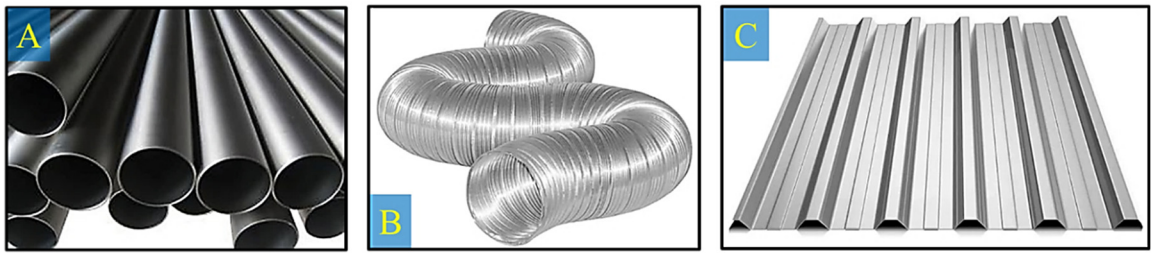

Figure 2. *Locally materials used for building the absorber: A) Aluminium tube absorber; B) Aluminium foil hose absorber; C) Trapezoidal steel plate absorber.*

Figure 3. *The SAH unit from different directions, highlighting the airflow inlet, outlet fan, and adjustable collector inclination.*

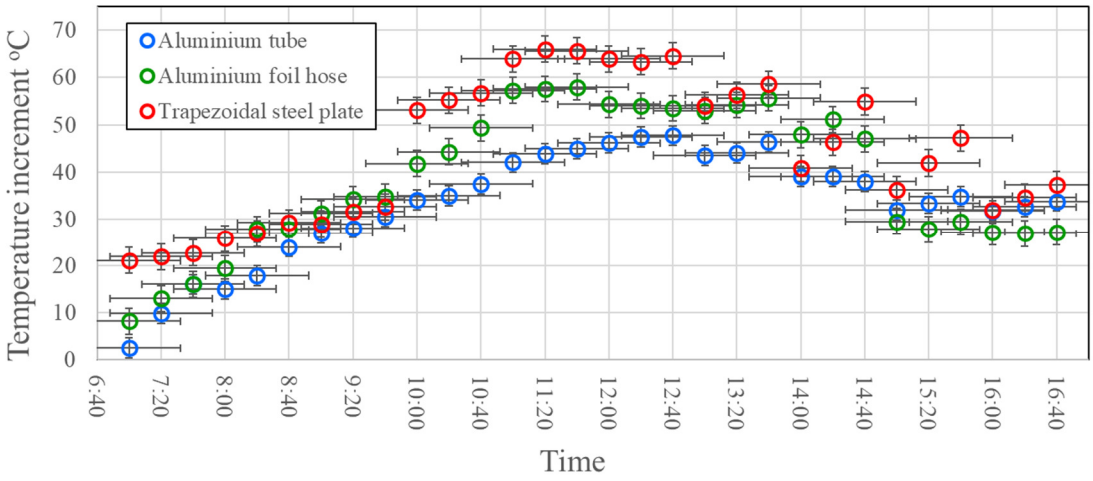

Figure 4. *Variation in air-temperature increment with time under natural convection for different absorber configurations.*

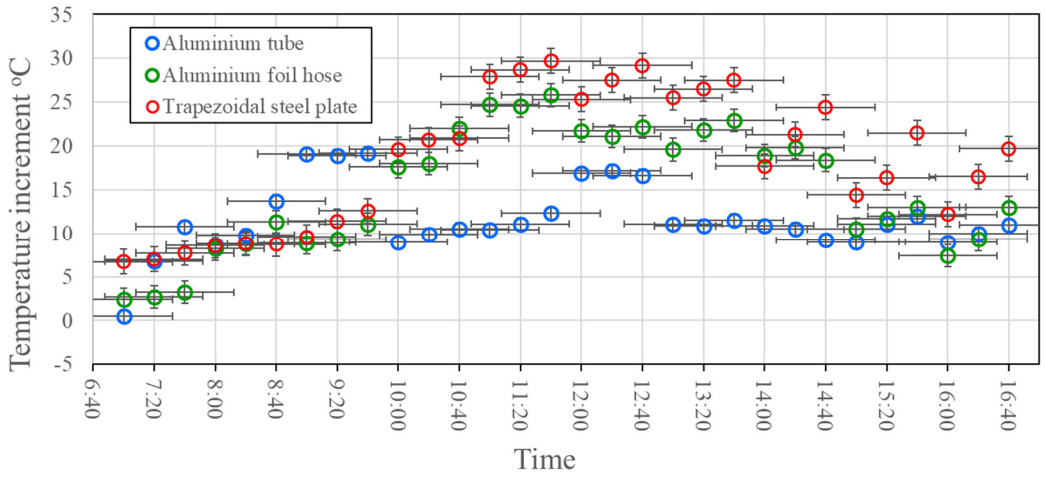

Figure 5. *Variation in air-temperature increment with time under forced convection for different absorber configurations.*

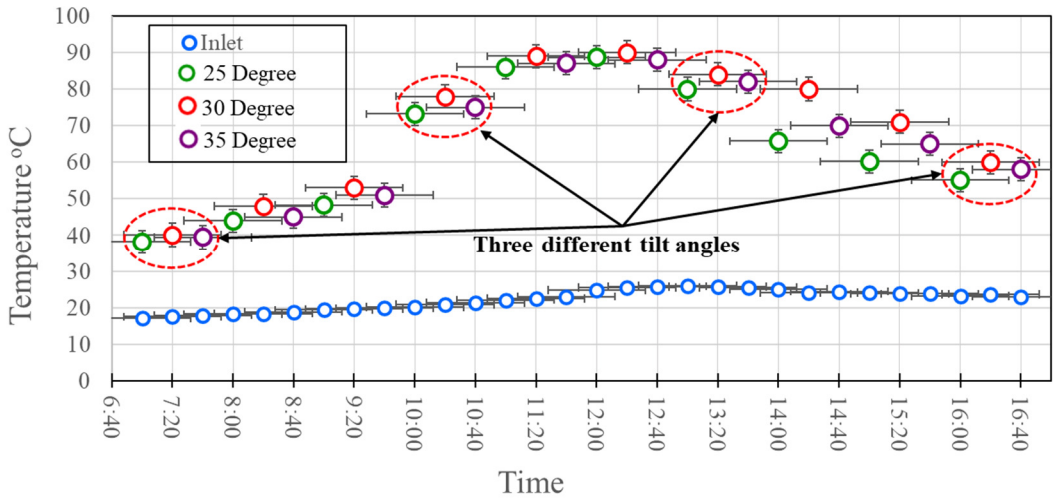

Figure. 6*. Variation of outlet-air temperature with time under natural convection for the trapezoidal steel plate absorber at three different tilt angles (25°, 30°, and 35°).*

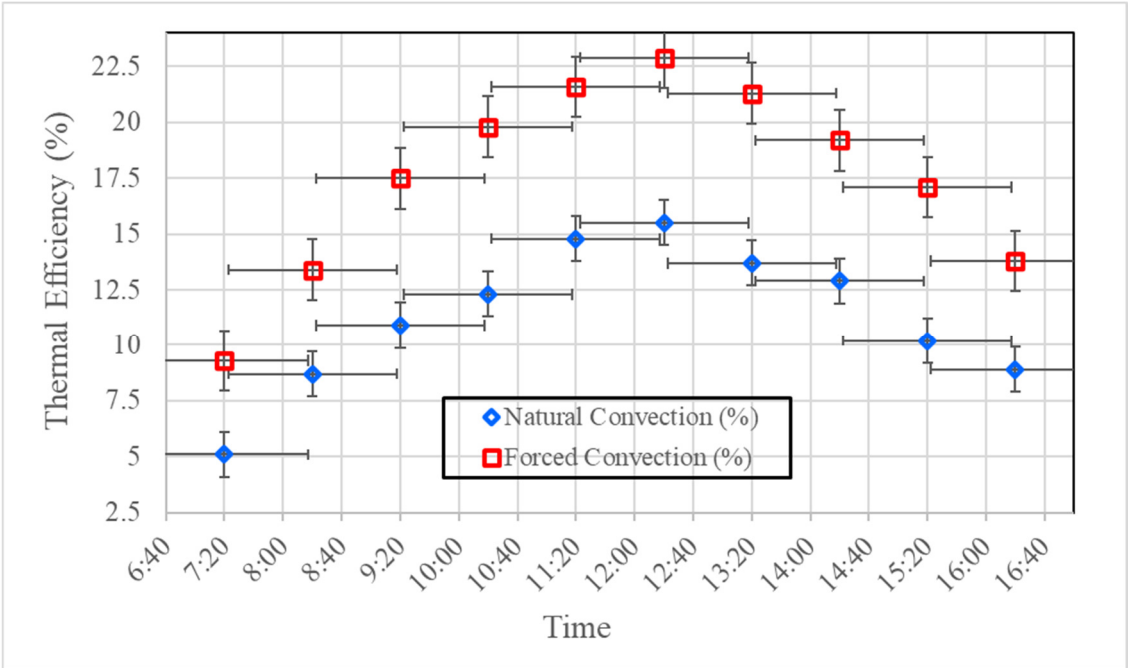

Figure 7. *Hourly variation of thermal efficiency under natural and forced convection modes for the trapezoidal steel absorber at a tilt angle of 30°.*

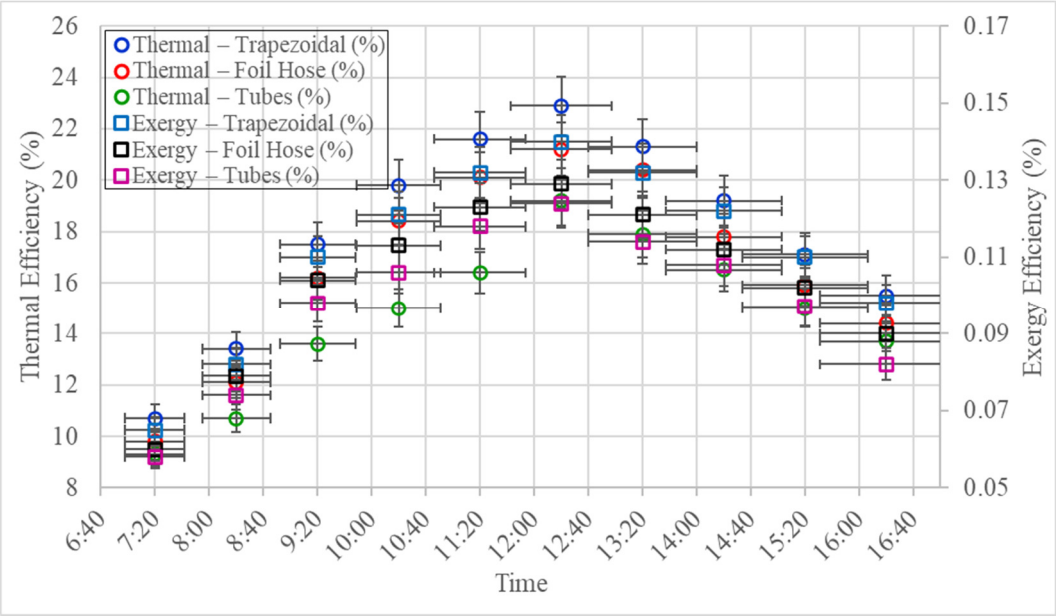

Figure 8. *Comparison of thermal and exergy efficiencies for three absorber geometries (trapezoidal steel plate, aluminium foil hose, and aluminium tubes) under forced convection at a tilt angle of 30°.*

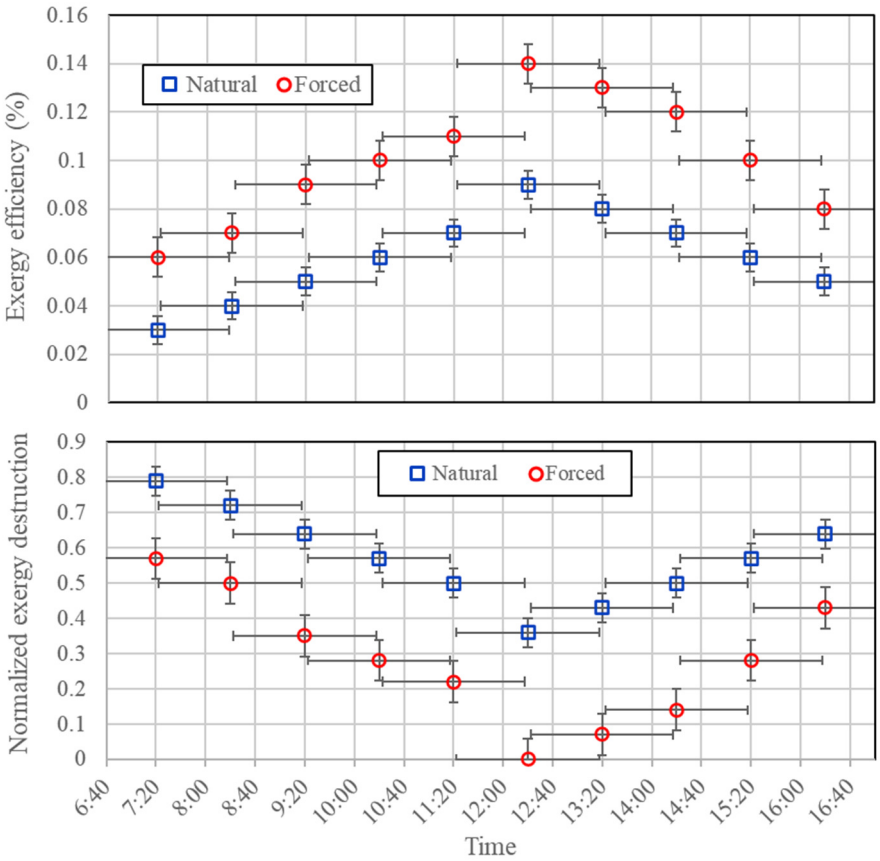

Figure 9*. Variation of exergy efficiency (top) and normalized exergy destruction (bottom) for the solar air heater under natural and forced convection throughout the daytime period at a 30° tilt angle.*

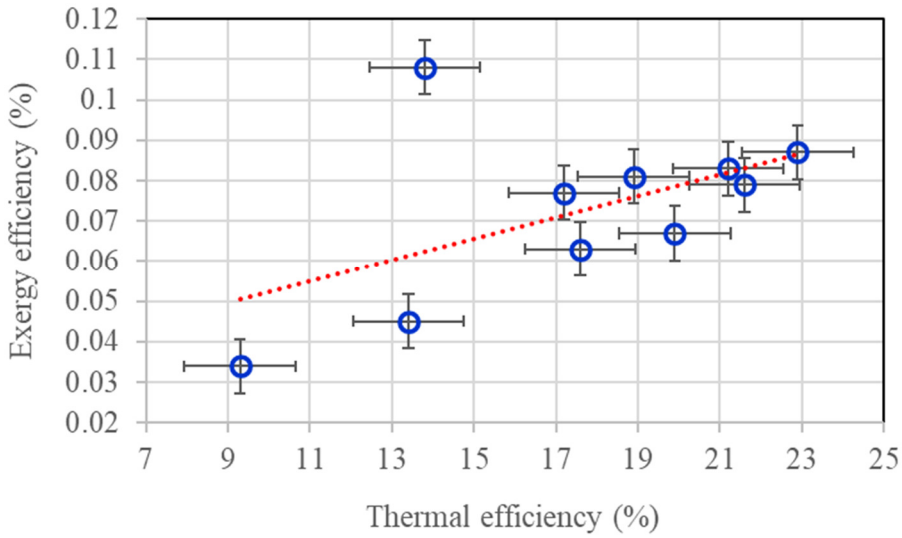

Figure 10. Correlation between thermal efficiency and exergy efficiency for the solar air heater equipped with the trapezoidal absorber under forced convection.

Table 1. *Key Parameters used in analytical evaluation. Source: the author*

Parameter	*Symbol*	*Value /Range*	*Unit*
Collector area	A	1.275	m^2
Tilt angles tested	–	$25°, 30°, 35°$	degrees
Inlet air temperature	T_{in}	$23 - 43$	℃
Effective sun temperature	$T_{\odot}$	5777	K
Outlet air temperature	T_{out}	$32 - 90$	–
Air velocity (forced mode)	V	$1.0 - 1.2$	m/s
Air density	ρ	$1.12 - 1.18$	kg/m^3
Specific heat of air	C_p	1.005	$kJ/kg.K$
Mass flow rate (forced mode)	–	$0.014 - 0.021$	kg/s

Table 2. Costs of materials and fabrication process for SAH prototypes

Components	Material	Quantity	Unit cost (USD)	Total cost (USD)
Collector frame	L-shaped steel	1 set	$15	$15
Glazing cover	4-5 mm clear glass	1 sheet	$10	$10
Insulation	Fiberglass blanket	1 roll	$5	$5
Interior wall lining	Plywood sheets	2 pieces	$9	$18
Absorber (type 1)	Aluminium tubes	10 tubes	$3	$30
Absorber (type 2)	Aluminium foil hoses	6 hoses	$4	$24
Absorber (type 3)	Trapezoidal steel sheet	1 sheet	$5	$5
Black matte paint	High-absorption coating	1 can	$5	$5
Fan (forced mode)	19 w axial fan	1 unit	$6	$6
Regulator	voltage speed controller	1 unit	$5	$5
Digital thermometer	-	1 unit	$12	$12
Airflow measurement	basic handheld	1 unit	$22	$22
Miscellaneous	wiring, brackets,	-	$20	$20